is the IIDF for a synchronous perturbation. Separating (6) into real and imaginary parts and eliminating Φ yields

$$(N_{re}+G_e)^2+(N_{je}+B_e)^2+A\frac{\partial N_{re}}{\partial A}(N_{re}+G_e)+A\frac{\partial N_{je}}{\partial A}(N_{je}+B_e)=0. \quad (7)$$

We observe that the border of stable locking determined by a synchronous perturbation is equivalent to

$$\frac{\partial A}{\partial \omega}=\infty \quad \text{or} \quad \frac{\partial \omega}{\partial A}=0$$

from (5).

This means that if A is plotted versus ω for a constant injected amplitude I_e, the locking becomes unstable just at the maximum frequency deviation (in those cases where such a maximum deviation exists); this was implicit in [4]–[6] but not explicitly stated. Note that we have no restrictions on the injected amplitude I_e or the frequency deviation, still the maximum frequency deviation determines a stable state, as long as such a maximum exists and lies in the region which is indicated as stable by the boundary curve(s). In view of the above we can restrict our study of stability to the use of nonsynchronous perturbations, which is usually an exceedingly simple matter; the border of stability is determined by [4, eq. (14) and (15)]:

$$N_{re}+G_e+\frac{A}{2}\frac{\partial N_{re}}{\partial A}=0 \quad (8)$$

$$N_{je}+B_e+\frac{A}{2}\frac{\partial N_{je}}{\partial A}=0. \quad (9)$$

The above discussion is illustrated in Figs. 1 and 2 where typical stability border curves are drawn for oscillators having nonlinear conductance and both nonlinear conductance and susceptance, respectively.

Van der Pol was aware of the rule concerning the locus curve for the particular oscillator which he studied. Since his method does not, however, allow for separation into different kinds of perturbations, this insight could not be practically applied.

The boundary curve is not necessarily single valued. It is, for instance, quite possible to have an oscillator which becomes stably locked when the amplitude crosses the lower boundary curve and then becomes unstably locked again if the injected power is increased so that the amplitude crosses the upper boundary curve.

It is to be noted that whereas the curves for constant injected amplitude are vertical at their intersections with the stability border determined by the synchronous perturbation ("the locus curve"), no such relationship exists regarding the stability border determined with nonsynchronous perturbations ("the boundary curve").

Our discussion has related to amplitudes; it is easily shown that identical relations can be established for the phase θ (i.e., $\partial\omega/\partial\theta=0$ at the border of stable locking determined by a synchronous perturbation). Concerning the output power it should be noted that $\partial A/\partial\omega\rightarrow\infty$ (synchronous stability border) corresponds to $\partial P_{out}/\partial\omega\rightarrow\infty$ provided that

$$N_{re}A+\frac{A^2}{2}\frac{\partial N_{re}}{\partial A}\neq 0.$$

Finally, it should be noticed that for an oscillator having a nonlinear susceptance it is very likely that the power required to bring an unlocked oscillator to a locked state for some frequencies exceeds that required to keep a locked oscillator in a locked state at the same frequencies. Our results pertain to the latter case. No information about the additional power required in the former case can be obtained by the use of synchronous and nonsynchronous perturbations.

The following simple rule has thus been established for the determination of the stable locking region ("holding" region) of an oscillator with a general tuning circuit. If, for a given injected amplitude, there exist points where $\partial\omega/\partial A=0$, these points determine the locking range, unless these points lie in the region which is unstable as determined by a nonsynchronous perturbation (8) and (9). This is valid irrespective of the magnitude of the frequency deviation from the free-running frequency. It should perhaps be pointed out that the technique described here can be used to study amplifiers as well, since the describing function introduced also describes an amplifier.

References

[1] M. J. E. Golay, "Normalized equations of the regenerative oscillator—Noise, phase-locking, and pulling," *Proc IEEE*, vol. 52, pp. 1311–1330, Nov. 1964.
[2] L. J. Paciorek, "Injection locking of oscillators," *Proc IEEE*, vol. 53, pp. 1723–1727, Nov. 1965.
[3] K. Kurokawa, "Some basic characteristics of broadband negative resistance oscillator circuits," *Bell Syst. Tech. J.*, vol. 48, pp. 1937–1955, 1969.
[4] G. H. B. Hansson and K. I. Lundström, "Phase locking of negative conductance oscillators," in *Proc. 1971 European Microwave Conf.*, pp. A6/4: 1–4.
[5] ——, "Stability criteria for phase-locked oscillators," *IEEE Trans. Microwave Theory Tech.*, vol. MTT-20, pp. 641–645, Oct. 1972.
[6] L. Gustafsson, G. H. B. Hansson, and K. I. Lundström, "On the use of describing functions in the study of nonlinear active microwave circuits," *IEEE Trans. Microwave Theory Tech.*, vol. MTT-20, pp. 402–409, June 1972.
[7] R. Adler, "A study of locking phenomena in oscillators," *Proc IRE*, vol. 34, pp. 351–357, June 1946.
[8] B. Van der Pol, "Forced oscillations in a circuit with nonlinear resistance," *Phil. Mag.*, vol. 3, pp. 65–80, Jan. 1927.

Broad-Band Twisted-Wire Quadrature Hybrids

R. E. FISHER

***Abstract*—A symmetrical 3-dB quadrature hybrid, consisting chiefly of a bifilar pair of twisted wires, is described. A cascade of two such hybrids can achieve an octave bandwidth with a 0.7-dB coupling error. Since this class of hybrid is simple, compact, and low in cost, its use may be preferred over the more common coaxial line or printed-circuit types in the frequency region below 1 GHz.**

I. Introduction

The concept of using twisted wires wrapped upon ferrite toroids to form compact, asymmetric, 180° hybrids was first introduced by Ruthroff [1]. It has also been found by several other investigators [2]–[4] that twisted-wire structures can be made to function as *symmetric*, 3-dB quadrature (90°) hybrids, thus permitting the construction of compact directional couplers at arbitrarily low frequencies.

Examples of twisted-wire quadrature hybrids centered at approximately 7 and 300 MHz are shown schematically and pictorially in Figs. 1, 2, and 5. For both hybrids, the coupling section consists of two strands of insulated copper magnet wire tightly twisted together to form a bifilar pair. For the 7-MHz hybrid shown in Fig. 2, the pair is wrapped upon a small ferrite toroid which is then soldered to four BNC along with two mica capacitors. For the 225–400-MHz two-stage hybrid shown in Fig. 5, where much less inductance is required, the wire pairs are bent into loops, and then soldered onto an epoxy fiberglass circuit board along with four omni-spectra-miniature (OSM) connectors.

II. Single-Stage Hybrid Design

Consider Fig. 1. If terminal 1 is connected to terminal 2, and terminal 3 is connected to terminal 4, the resulting two-terminal network is now simply a lumped inductance L, since the magnetic coefficient of coupling between the twisted wires is nearly unity.

If terminal 1 is connected to terminal 4, and terminal 2 is connected to terminal 3, this different two-terminal network can be approximated by a lumped capacitor C, which is the sum of the interwinding capacitance and the external capacitors. At UHF, the external capacitors may not be required.

The 4-port will display hybrid properties when

$$Z_0=\sqrt{\frac{L}{C}}. \quad (1)$$

Equal power division between ports 2 and 4 will occur at a frequency f_0 where

$$\omega_0 L=\frac{1}{\omega_0 C}=Z_0$$

$$\omega_0=2\pi f_0. \quad (2)$$

The transducer loss between ports 1 and 2 is

$$\frac{P_1}{P_2}=1+\left(\frac{\omega_0}{\omega}\right)^2 \quad (3)$$

Manuscript received May 1, 1972; revised November 8, 1972.
The author is with Bell Laboratories, Whippany, N. J. 07981.

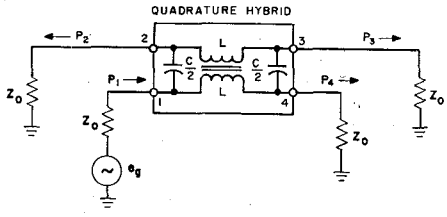

Fig. 1. Quadrature-hybrid functional diagram.

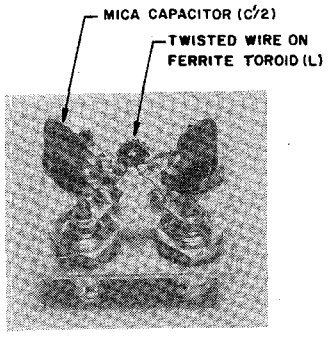

Fig. 2. Photograph of 7-MHz quadrature hybrid.

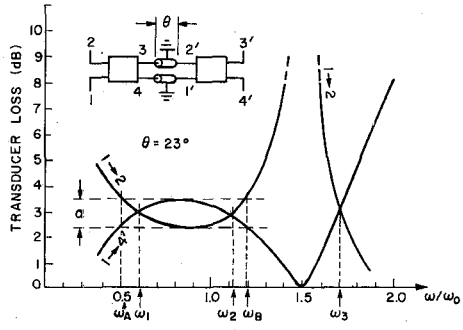

Fig. 3. Computer-generated characteristics of two-stage quadrature hybrid when $\theta = 23°$.

and between ports 1 and 4 is

$$\frac{P_1}{P_4} = 1 + \left(\frac{\omega}{\omega_0}\right)^2. \tag{4}$$

The port 3 isolation and return loss (at all ports) is theoretically infinite at all frequencies. Also, the voltages at ports 2 and 4 should differ in phase by 90° over an infinite frequency band.

The 7-MHz hybrid shown in Fig. 2 exhibited a measured insertion loss of 0.1 dB, and the isolation and return loss both exceeded 30 dB. One stage of the 300-MHz dual hybrid shown in Fig. 5 had a measured insertion loss of 0.2 dB, while the isolation and return loss were about 20 dB.

III. Broad-Banding the Hybrid

Equations (3) and (4) indicate that a single-stage twisted-wire quadrature hybrid is not a very broad-band network, since equal power division occurs only at one frequency.

However, the hybrid can be broad-banded by cascading two sections, as shown in Fig. 3. Ports 3 and 4 of the first hybrid are connected, respectively, to ports 1′ and 2′ of the second identical hybrid via sections of Z_0 coaxial cable each having an electrical length θ at ω_0.

When this two-stage cascade was computer analyzed,[1] it exhibited the transmission characteristics shown in Fig. 3. All frequencies are normalized to ω_0, which is the 3-dB frequency of each hybrid used in the cascade. Note that there exist three frequencies ω_1, ω_2, and ω_3 where equal division of generator power occurs. The frequencies

[1] The computer program used was BELNAP-II, a Bell Laboratories linear circuit-analysis program.

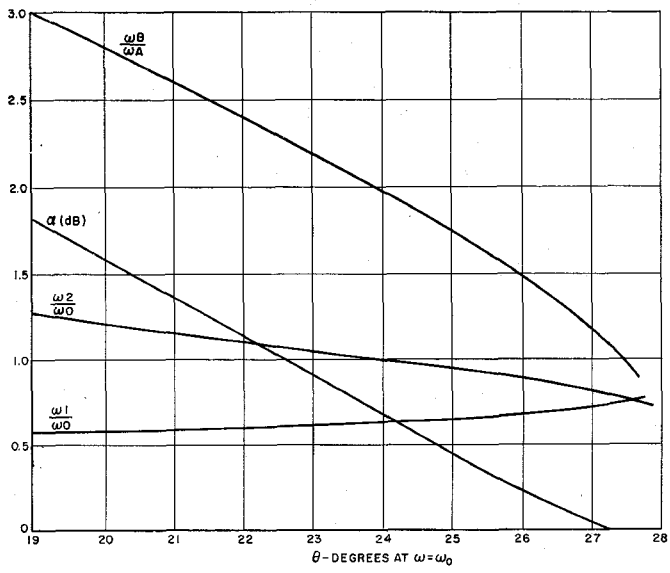

Fig. 4. Two-stage quadrature-hybrid transmission parameters versus connecting cable length.

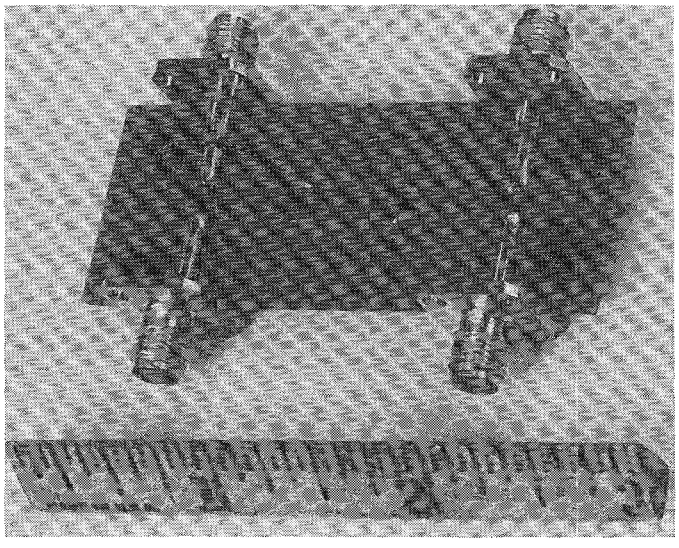

Fig. 5. Photograph of two-stage 225–400-MHz quadrature hybrid.

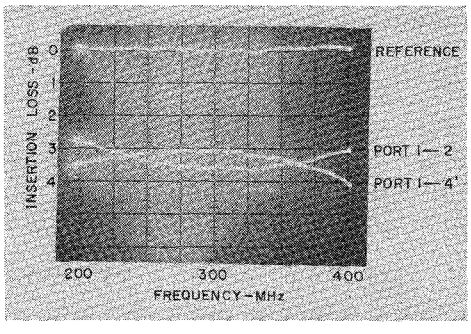

Fig. 6. Measured characteristics of two-stage 225–400-MHz quadrature hybrid.

ω_A and ω_B define that frequency band over which the difference in coupling never exceeds α.

Fig. 4 presents some graphs which can be used to design a broad-band two-stage hybrid. These show how some of the transmission characteristics given by Fig. 3 are related to the electrical length of the connecting cables. An octave bandwidth ($\omega_B/\omega_A = 2$) results when $\theta \cong 24°$. Over this band the coupling difference α will never exceed 0.7 dB.

Figs. 5 and 6 show, respectively, the photograph and transmission characteristics of a two-stage hybrid designed to cover the 225–400-MHz communications band. Note that α is about 0.5 dB, which implies from Fig. 4 that the coupling lines are about 24.7° long. The isolation and return loss exceeded 20 dB over the measured band. The insertion loss never exceeded 0.5 dB.

An apparent disadvantage of this cascade technique is that the coaxial connecting cables become prohibitively long as the hybrid operating frequency is lowered. This problem can be bypassed by substituting lumped-element low-pass filters for the coaxial cables.

References

[1] C. L. Ruthroff, "Some broad-band transformers," *Proc. IRE*, vol. 47, pp. 1337–1342, Aug. 1959.
[2] W. L. Firestone, U.S. Patent 2 972 121, Feb. 1961.
[3] K. Kurokawa, "Design theory of balanced transistor amplifiers," *Bell Syst. Tech. J.*, vol. XLIV, no. 8, pp. 1675–1698, Oct. 1965.
[4] J. D. Cappucci and H. Seidel, U.S. Patent 3 452 300 and 3 452,301, June 1969.

Resolution of the Paradox Concerning Energy Flow on Nonlinear Transmission Lines

A. E. KARBOWIAK AND R. H. FREEMAN

***Abstract*—The energy relations and the constitutive relations pertaining to a nonlinear transmission line are examined in detail. It is concluded that mathematical models which have been used in certain studies and which lead to the paradox concerning energy dissipation in the shock front are inadmissible. Correct models are free from such paradoxes. The work leads to the formulation of the hypothesis of realization: it is impossible to realize a continuous loss-free transmission medium which would be characterized by nonlinear distributed inductance $L(I)$ and capacitance $C(V)$, unless the medium is dispersive.**

Introduction

It is well known from studies in gas dynamics [1] that wave propagation in a nonlinear medium is accompanied by formation of shock waves. More recently, Landauer [3] and Riley [4] carried out similar studies with respect to an electrical nonlinear transmission line. Their work confirms the existence of shock wave and energy dissipation in the vicinity of the shock front. However, with electrical transmission lines it is possible, at least in principle, to reduce the dissipation in the resistive elements to zero, and then, of course, it becomes difficult to account for the energy lost.

To explain the paradox, some argue that the problem is improperly formulated and that the model must contain resistive elements [3], while others suggest that the lost energy is radiated from the system by electromagnetic means [4]. Such "explanations," however, are not tenable; if the system is screened, like a coaxial cable, radiation cannot be evoked. The problem with postulating resistive elements is that if the problem is to be properly formulated, then it must be possible to obtain a valid solution in the limit as the resistive elements are reduced to zero. This, however, is not the case. When the resistive elements are sufficiently small, the rate of energy loss in the shock region is much too slow (in the limit infinitely slow) to account for the loss implied.

The purpose of this short paper is to resolve the paradox, as far as distributed systems are concerned, through a detailed study of the equations involved.

Mathematical Model

If we accept the validity of Maxwell's equations, then we must also accept the pair of equations

$$\frac{\partial V}{\partial x} = -L(I)\frac{\partial I}{\partial t} \tag{1a}$$

$$\frac{\partial I}{\partial x} = -C(V)\frac{\partial V}{\partial t} \tag{1b}$$

Manuscript received May 8, 1972; revised July 14, 1972.
The authors are with the School of Electrical Engineering, University of New South Wales, Kensington, New South Wales, Australia.

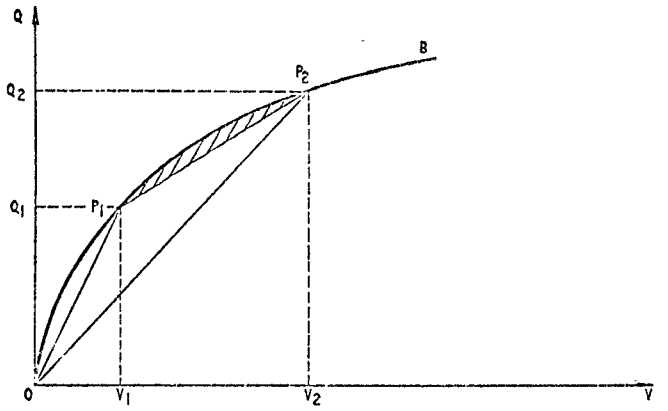

Fig. 1. Charge–voltage relation for a nonlinear capacitor.

describing voltage (V) and current (I) on a nonlinear transmission line.

The functions $C(V)$ and $L(I)$ are the constitutive relations describing the properties of the materials making up the transmission line. These describe, respectively, the differential capacitance and inductance per unit length. For a nonlinear capacitor, the charge Q as a function of voltage V can be represented by the nonlinear relation $Q=Q(V)$ and the capacitance (really an incremental capacitance) is defined by $dQ/dV=C(V)$. We may regard $C(V)$ as a physical property of the nonlinear capacitor.

In a similar way for a nonlinear inductor we have $\phi=\phi(I)$, where ϕ is the magnetic flux and the nonlinear inductance is defined by $L(I)=d\phi/dI$.

Fig. 1 shows a convex relation for a nonlinear capacitor and *mutatis mutandi* a similar curve would apply with reference to a nonlinear inductance with the one-to-one correspondence $(\phi, L, I) \sim (Q, C, V)$.

It is sufficient to consider a particular relation, such as convex, for the following reason.

From studies in fluid dynamics, it is known that for a convex relation between the velocity of propagation and the amplitude of the disturbance, the trailing edge of the disturbance disperses while the leading edge becomes a "shock front," whereas for a concave relation it is the leading edge that disperses and the trailing edge becomes the shock front. In this short paper we are concerned with energy-conversion processes at the shock front as normally understood, and whether the relations are convex or concave the results are the same.

Energy Conservation

We now examine the energy conservation in a region containing a disturbance which forms a transition from V_1, I_1 on one side to V_2, I_2 on the other. If u is the velocity of the disturbance (to be determined) and since charge and magnetic flux must be conserved, we can equate the rate of accumulation of charge in the region, that is $u(Q_2-Q_1)$, to the net current influx, that is I_2-I_1. A similar reasoning applies with respect to the magnetic-flux (ϕ) conservation, that is, $u(\phi_2-\phi_1)$ must be equal to V_2-V_1. In this way we get

$$u(Q_2 - Q_1) = I_2 - I_1 \tag{2a}$$

and

$$u(\phi_2 - \phi_1) = V_2 - V_1. \tag{2b}$$

Equations (2a) and (2b) determine uniquely the velocity of the disturbance.

The apparent energy loss in the vicinity of the disturbance can be calculated as a difference between the net energy influx and the increase in stored energy. The net rate of energy influx is $V_2I_2-V_1I_1 = \frac{1}{2}[(V_2+V_1)(I_2-I_1)+(I_2+I_1)(V_2-V_1)]$, while the rate of increase in stored magnetic and electric energies is $u\int_{\phi_1}^{\phi_2} I\,d\phi$ and $u\int_{Q_1}^{Q_2} V\,dQ$, respectively, u being the velocity of propagation.

The total rate of energy loss is

$$P = u\left\{\left[\tfrac{1}{2}(V_2+V_1)(Q_2-Q_1) - \int_{Q_1}^{Q_2} V\,dQ\right] + \left[\tfrac{1}{2}(I_2+I_1)(\phi_2-\phi_1) - \int_{\phi_1}^{\phi_2} I\,d\phi\right]\right\}. \tag{3}$$